Heliyon 9 (2023) e18179

Contents lists available at ScienceDirect

Heliyon

journal homepage: www.cell.com/heliyon

Anatomical characterization of the intraosseous arteries of the porcine tibia

Jiaming Wan [a,1], Hongyu Wang [b,1], Dingsong Wang [b], Xiaosong Wang [b], Ruixing Hou [a,c,*]

[a] Yangzhou University Medical College, Yangzhou, China
[b] Suzhou Medical College of Soochow University, Suzhou, China
[c] Suzhou Ruihua Orthopedic Hospital, Suzhou, China

ARTICLE INFO

Keywords:
Porcine
Corrosion
Intraosseous artery
Tibia
Safe corridor

ABSTRACT

Introduction: Tibial fractures have a high rate of post-fracture complications. Blood supply is recognized as a positive factor in tibial fracture healing. However, it's difficult to assess blood supply damage after tibial fracture because of the lack of understanding of the tibial intraosseous arteries. This study aimed to delineate and anatomically characterize porcine tibial intraosseous arteries, as a model for the human system.

Methods: Twenty right calf specimens with popliteal vessels were prepared from ordinary Landrace pigs. Epoxy resin was perfused into the vasculature from the popliteal artery. After 24 h, casts of the intraosseous arteries of the tibia were exposed through acid and alkali corrosion. The distribution and anatomy of the exposed intraosseous arteries were observed and measured under a microscope, and the data were statistically analyzed.

Results: Sixteen complete specimens were obtained. The medullary artery bifurcated into the main ascending and descending branches, which each split into two upward primary branches that further divided into 1–3 secondary branches. Among all specimens, 56 ascending and 42 descending secondary branches, which were all $\geq$0.3 mm in diameter. Furthermore, the horizontal plane was divided into three zones—safety, buffer, and danger zones—according to the probability of the presence of intraosseous artery.

Discussion: The cast perfusion and corrosion approach was successfully applied for anatomical characterization of the intraosseous arteries of the porcine tibia. These observations provide a theoretical basis for understanding the tibial vasculature in humans and will facilitate the establishment of novel "safe corridor" in the tibia for the protection of the blood supply during surgery.

1. Introduction

Tibial fractures have among the highest post-fracture complication rates and can have a wide-ranging impact on the lives of affected patients [1]. Given the diversity of injury mechanisms, tibial fractures can occur at any age and in any situation [2]. In the

* Corresponding author. Yangzhou University Medical College, Yangzhou, China.
E-mail address: hrx2023@126.com (R. Hou).
[1] JW and HW contributed equally to this work.

https://doi.org/10.1016/j.heliyon.2023.e18179
Received 16 March 2023; Received in revised form 6 July 2023; Accepted 10 July 2023
Available online 11 July 2023

United States alone, the annual economic loss from tibial fractures was approximately $1.4 billion [3].

Factors that affect the healing of tibial fractures have been extensively investigated. Although some of the results are controversial, it is widely recognized that blood supply plays a positive role in the tibial healing process [4], especially in the early stages, which are characterized by hematoma and inflammatory reactions [5,6]. However, it is difficult to accurately assess the extent of blood supply injury in different fracture types, owing to an incomplete understanding of the tibial vasculature.

Based on techniques, such as anatomical observation and microangiography, the distribution of the feeding arteries of the tibia can be divided into extraosseous and intraosseous regions. The distribution of extraosseous arteries can be easily observed and is well-described [7,8]. Accordingly, "safe corridor" for external fixation devices can be designed to avoid damage to important structures, including the posterior tibial artery and nerves [9,10]. The intraosseous artery encompasses a greater proportion of the blood supply to the tibia than the external artery [11]. However, given the lack of direct visual detection methods, the distribution of the intraosseous arteries remains largely unknown. This not only affects the assessment of the degree of blood supply injury after tibial fracture but also leads to unavoidable iatrogenic injury to the intraosseous artery.

To facilitate observation and measurement of the intraosseous arteries, the bone and soft tissue around the arteries should be removed. Owing to the calcified structure of the tibial cortex, maintaining the integrity of the intraosseous arteries while removing the cortex has proven to be challenging. Zhang et al. [12] used a casting agent perfusion and corrosion method to generate femoral head specimens in which the intraosseous arteries were exposed, and achieved satisfactory results. According to previous studies, pig tibia are considered suitable substitutes for studying human tibia due to their similarities in anatomy and vascular distribution [13,14]. Accordingly, the aims of this study were to expose the porcine tibial intraosseous arteries using similar methods, quantify the number and describe the spatial distribution of the tibial intraosseous arteries, and provide a theoretical basis for understanding the tibial vasculature and establishing the concept of new "safe corridor" for the protection of the tibial intraosseous blood supply during surgery. This study aimed to achieve this goal.

2. Materials and methods

2.1. Materials

The study protocol was approved by the Institutional Animal Care and Use Committee, Suzhou Ruihua Orthopedic Hospital, Suzhou, China (Approval number: RHGK2023013). Twenty right-calf specimens with popliteal vessels (ordinary Landrace pigs, male, mean age:10 months, weighing approximately 150 kg) were harvested from a licensed slaughterhouse. The epoxy resin (Dongguan Xiaoma New Material Technology Co., Ltd., No. 318AB-C2-1 kg) included solution A colloid (($C_{11}H_{12}O_3$)n) and solution B diluent ($C_3H_{10}N_2O$). Other experimental materials and equipment included a manometer (SanLiang, DP370), UV-curing adhesive (Kisling AG, ergo8500), dual-viewing optical microscope (Zhenjiang Zhuochuang Medical Technology Co., Ltd., AC220V/50 Hz), annular angle square (Hengjiu Wanfeng, A024), and micro-scale laser generator (DeLi, 3933).

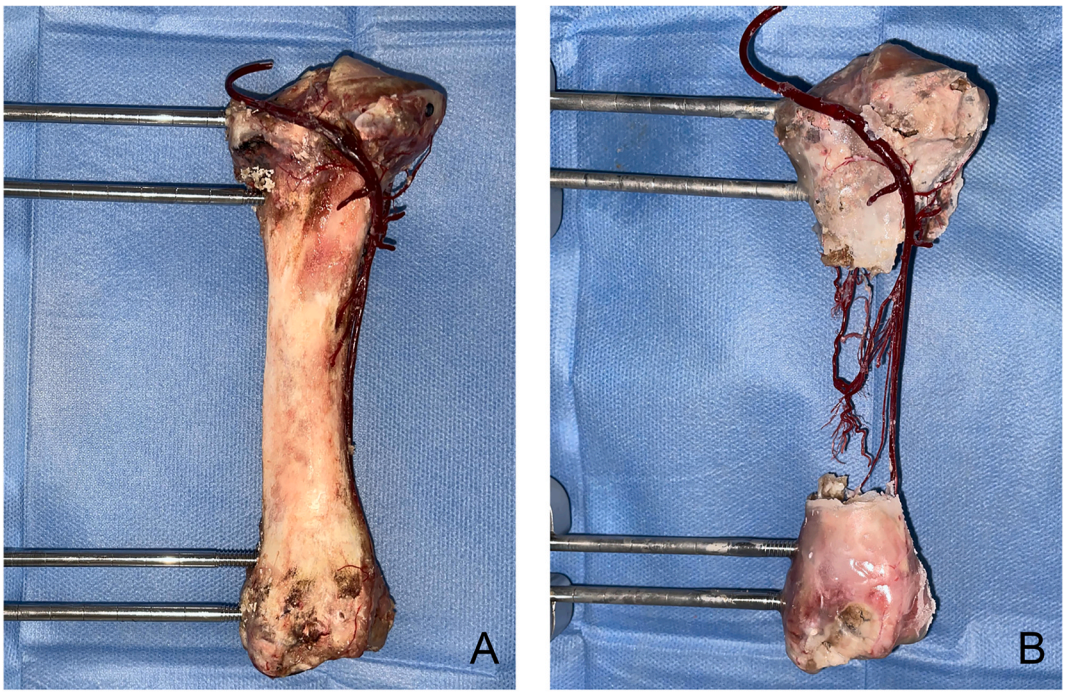

Fig. 1. Intraosseous vascular cast. A. After NaOH corrosion; B. After HCl corrosion.

2.2. Vascular casting

Solutions A and B were mixed in a weight ratio of 3:1 with four drops of red metal complex dye [12]. The mixture was thoroughly mixed and left for 30 min to eliminate air bubbles.

The popliteal artery was dissected from the specimen, and an indwelling needle hose with the needle removed was inserted and securely fixed using a silk thread. Heparin saline (625 U/mL) was injected into the popliteal artery to wash the blood remaining in the vessel and observe vascular branches in the distal calf. After flushing, the distal branch vessels were ligated [12], while preserving the posterior tibial artery. A syringe, manometer, and indwelling needle were connected sequentially, and the epoxy resin fluid was perfused at a constant pressure of 25 KPa [15]. Care was taken to prevent air from entering the sealed system. When red epoxy could be seen at the stump of the posterior tibial artery, the indwelling needle and the posterior tibial artery were ligated, and then a small amount of epoxy was re-infused at 15-min intervals to keep the popliteal artery full. Perfusion was terminated after 3 h.

After 24 h, the muscles around the tibia were removed using a scalpel and soaked in 50% NaOH solution for 6 h to remove soft tissue from the surface of the tibia (Fig. 1A). A total of four 5.0-mm-diameter pins were implanted at 1.5 cm and 2.0 cm below the tibial plateau, and 1.5 cm and 2.0 cm above the ankle plane, with the anterior edge of the tibia as the landmark line, and the pins were connected with an external fixation brace. A UV-curing adhesive was applied to cover the bone pins and the surrounding bone surface to prevent loosening of this part through acid and alkaline corrosion. After soaking in 10% HCl solution, the softened impurities were peeled off from the tibia under a microscope at 12-h intervals to gradually expose the intraosseous arteries [16] (Fig. 1B).

2.3. Data measurement

When the intraosseous arterial casts were completely exposed, the distribution pattern and anastomosis of the intraosseous arteries were observed under a microscope, and the caliber was measured to identify vessels with a diameter greater than or equal to 0.3 mm [17]. The tibia was fixed vertically, and the spatial distribution range of each vessel was measured and recorded using an annular angle square and laser generator (Fig. 2A–C).

2.4. Statistical analysis

The data obtained were analyzed using SPSS software (version 21.0; IBM SPSS Statistics for Windows, Jiangsu, Suzhou, China) and are expressed as mean ± standard deviation (SD).

3. Results

3.1. Clear cast specimens of the intraosseous tibial artery

After acid–base corrosion, 16 complete specimens (4 were excluded due to perfusion failure) with an average height of 16.2 ± 2.7 cm were obtained from the cast of the intraosseous tibial artery. Among the specimens, only one had two ascending branch trunks and

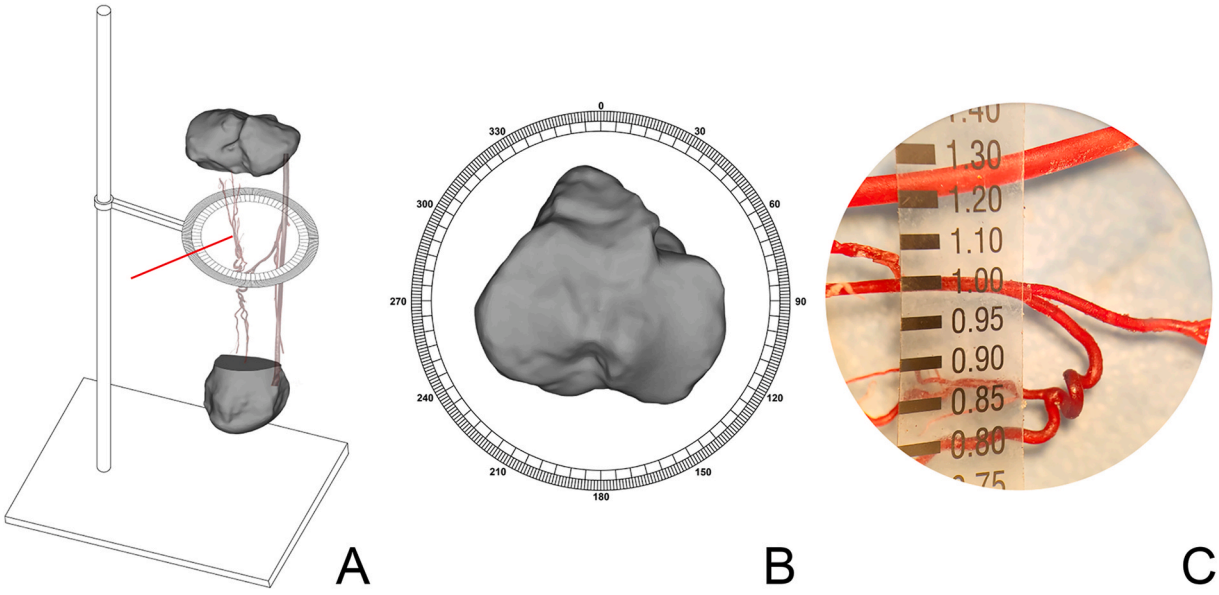

Fig. 2. Data collection. A. Vascular data measurement methods (red indicates laser). B. Vascular angle measurement; C. Vascular diameter measurement.

one descending branch trunk (Fig. 3A), whereas the remainder had one ascending trunk and one descending branch trunk (Fig. 3B).

3.2. Number and diameter of intraosseous arteries

The medullary artery branches into main ascending and descending branches. The main ascending branch split into two upward primary branches and main descending branch split into two downward primary branches (Fig. 4A and B), each of which was further divided into one to three secondary branches (Fig. 4C and D). Among all specimens, there were 56 ascending secondary branches and 42 descending secondary branches measuring ≥0.3 mm.

In all specimens, 16 medullary arteries with a mean diameter of 0.99 ± 0.14 mm were collected, including 17 main ascending branches, 16 main descending branches, 56 ascending branches, and 42 descending branches with a mean diameter of 0.85 ± 0.11 mm, 0.86 ± 0.1 mm, 0.56 ± 0.09 mm, and 0.57 ± 0.11 mm, respectively (Table 1).

3.3. Spatial distribution of intraosseous arteries

According to the segment of the tibia reported by Nayagam [10] and the observations in this study, the intraosseous arteries in the interepiphyseal region of the tibia on the proximal and distal sides were fully exposed and divided into three zones: ascending, parallel, and descending, from proximal to distal. The parallel zone was located near the midpoint of the full length of the tibia, with an average height of 1.6 ± 0.7 cm. In this zone, the medullary artery divides into ascending and descending arterial trunks, and the trunk artery branches out to the proximal and distal sides after winding for some distance. The ascending and descending zones are located between the proximal and distal tibial epiphysis and the upper and lower edges of the parallel zone, with an average height of 5.6 ± 1.8 and 4.5 ± 1.4 cm, respectively (Fig. 5).

The medullary artery is divided into 1–2 ascending arterial trunks and 1 descending arterial trunk near the middle tibial segment. The ascending trunk travels a short distance in the same plane and then divides into two ascending branches, each of which again branches into one or three secondary branches. The latter are mostly twisted and loose, and are connected by traffic branches, forming a circular anastomosis and converging into the proximal tibia. The descending trunk is long and straight and travels downward in the medullary cavity for a distance, after which it splits into two downward branches, each of which is again divided into one to three tree-like secondary branches that converge into the distal tibia. Some of the branches near the inner surface of the bone cortex emit capillaries that penetrate the bone cortex and anastomose with the extracortical periosteal artery branches. In general, the distribution characteristics of the intraosseous artery in the porcine tibia were as follows: 1) Most of the branches of the intraosseous artery were distributed in a discrete manner along the inner surface of the bone cortex, while a few were coiled in the center of the medullary cavity; 2) except for the arterial trunk, branching was more extensive in the posterior than in the anterior of the intraosseous artery, and there were more internal than external branches.

The paths of all vessels with a diameter greater than or equal to 0.3 mm in regions containing ascending and descending branches were also recorded (Tables 2 and 3, Fig. 6A and B). We divided the horizontal plane according to the probability of the presence of the intraosseous artery and defined the interval with fewer than four arterial courses (<4/16, probability <25%) in the 16 specimens as the safety zone, the interval with four to eight arterial courses (4–8/16, ≥25% probability <50%) as the buffer zone, and the interval with eight or more arterial courses (≥8/16, probability ≥50%) as the danger zone (Fig. 7A–C). The safety zone in the ascending branch region was concentrated in the range of 340–100°, with a scattered distribution in other regions. In contrast, the danger zone in this

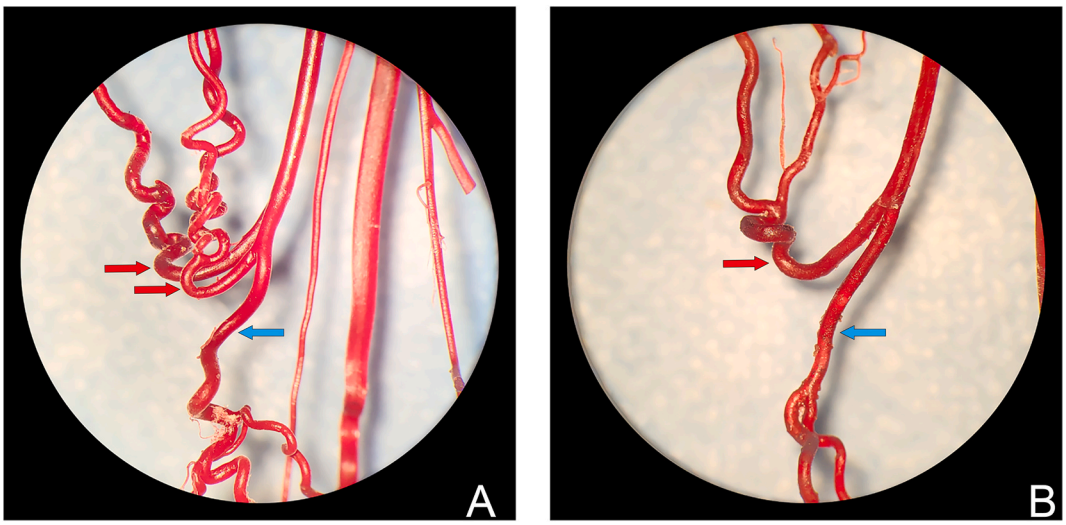

Fig. 3. Microscopic observation of main intraosseous blood vessel. Red arrow indicates ascending branch, and blue arrow indicates descending branch. A. Special form of two ascending branches; B. Regular form of one ascending branch.

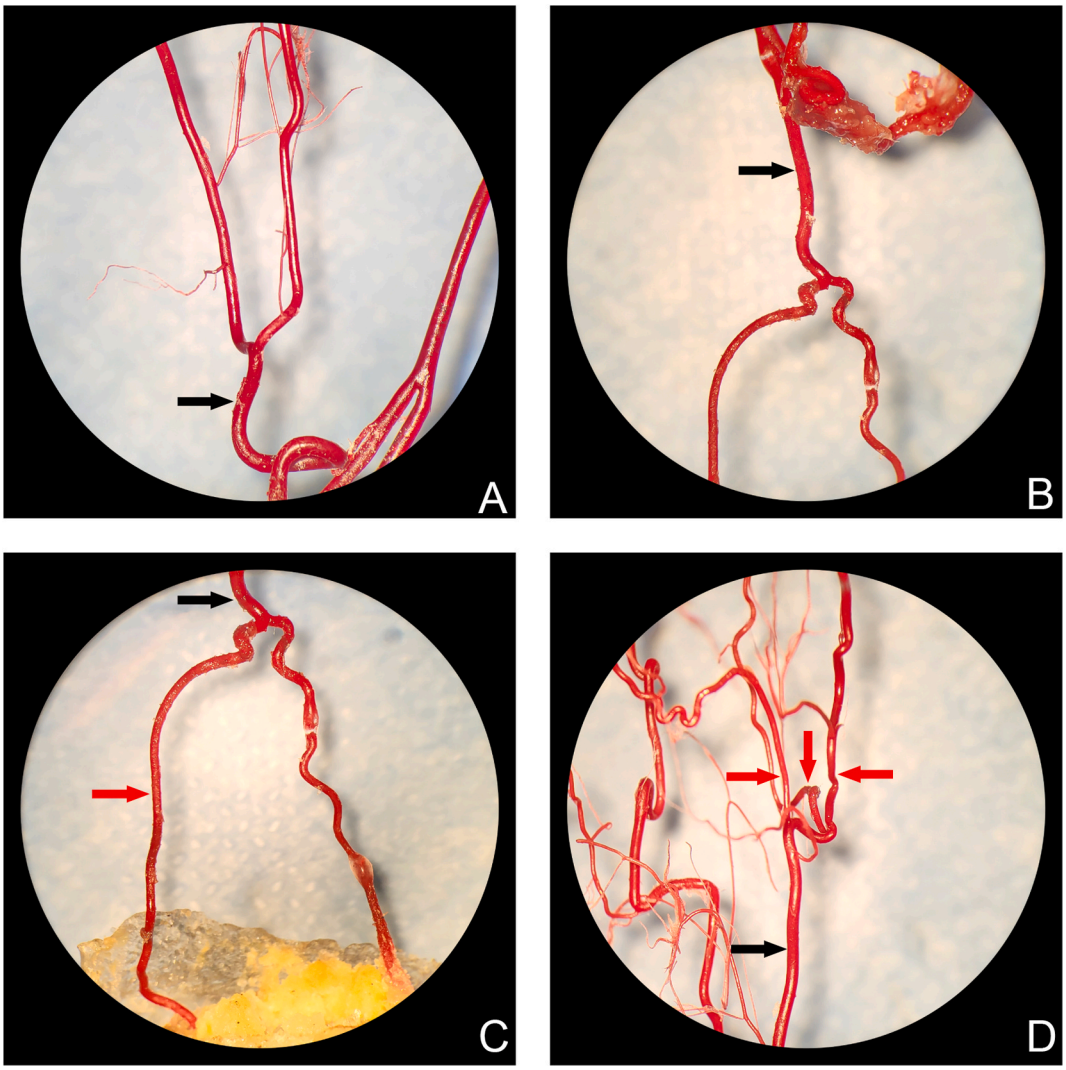

Fig. 4. Number of intraosseous artery branches. Black arrow indicates the primary branch, red arrow indicates the secondary branch. A. Primary branch of main ascending branch; B. Primary branch of main descending branch; C. Primary branch gives rise to one secondary branch; D. Primary branch gives rise to three secondary branches.

Table 1
Diameter (mm) of intraosseous blood vessels.

Item	*n*	Max	Min	Mean ± SD
Main medullary artery branch	16	1.20	0.70	0.99 ± 0.14
Main ascending branch	17	1.10	0.70	0.85 ± 0.11
Main descending branch	16	1.00	0.65	0.86 ± 0.10
Ascending branch	56	0.75	0.35	0.56 ± 0.09
Descending branch	42	0.80	0.40	0.57 ± 0.11

Max and Min refer to the maximum and minimum diameter in one single tibia, respectively.

region was concentrated in the range of 210–280°. The safety zone in the descending branch region was concentrated in the range of 300–85°, with a small distribution in the posterior lateral tibia, whereas the danger zone of the descending branch region was concentrated in the range of 180–250°. The other intervals met the criteria for a buffer zone.

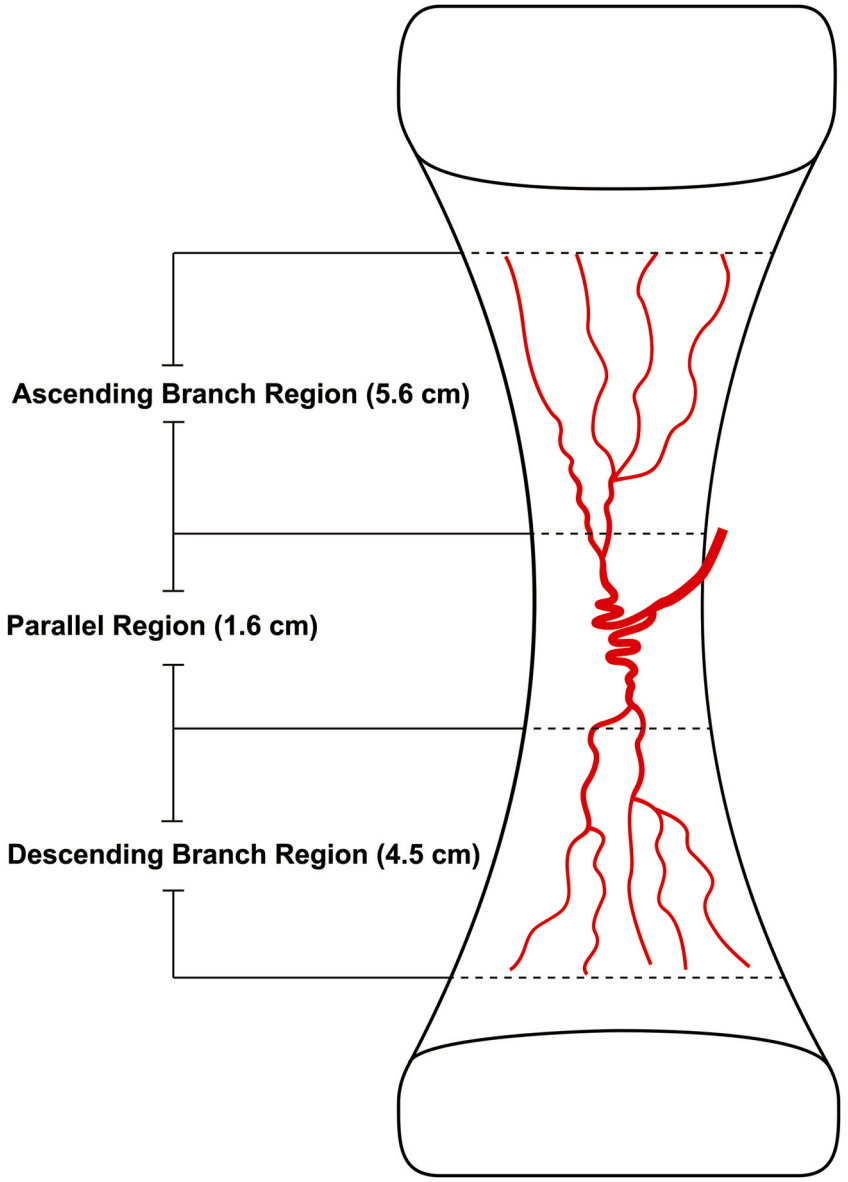

Fig. 5. Schematic diagram of intraosseous vessels.

Table 2
Number of vascular distribution.

Item	Distribution area		
	Medial	Lateral	Both
Ascending branch	37	13	6
Descending branch	29	8	5

Medial and Lateral correspond to the locations of the tibial vascular distribution in Fig. 6. Medial: 180°–360°; Lateral: 0°–180°.

4. Discussion

4.1. The choice of experimental materials

This study aimed to generate tibial specimens exposed to the intraosseous artery to investigate the pattern of distribution and

Table 3
Vascular distribution angle size (°).

Item	Medial			Lateral		
	Maximum	Minimum	Average	Maximum	Minimum	Average
Ascending branch	105	1	31.66 ± 24.93	42	1	16.11 ± 14.30
Descending branch	102	2	31.10 ± 28.37	130	30	68.13 ± 41.05

Medial and Lateral correspond to the locations of the tibial vascular distribution in Fig. 6. Medial: 180°–360°; Lateral: 0°–180°.

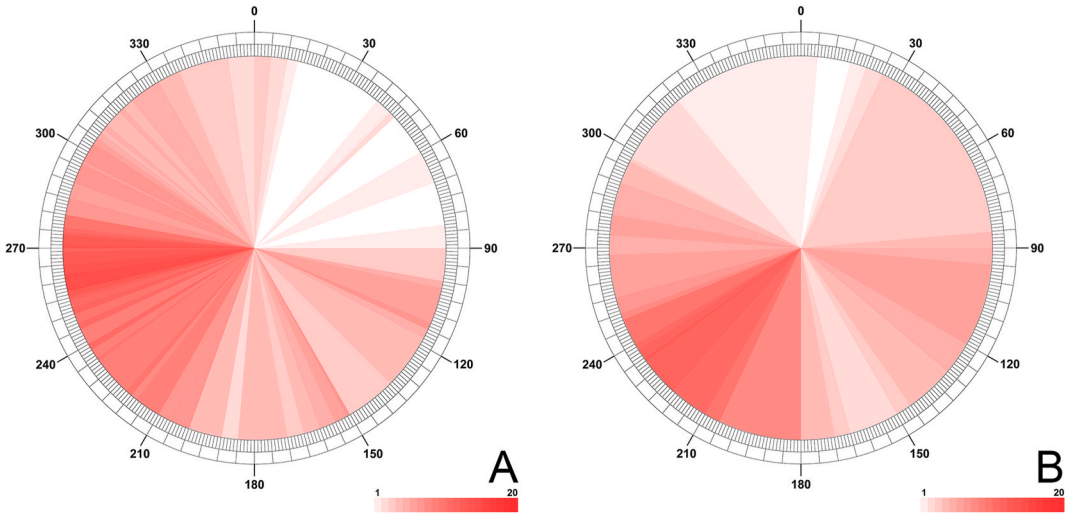

Fig. 6. Distribution range of intraosseous arteries. A. Distribution range of ascending branch; B. Distribution range of descending branch.

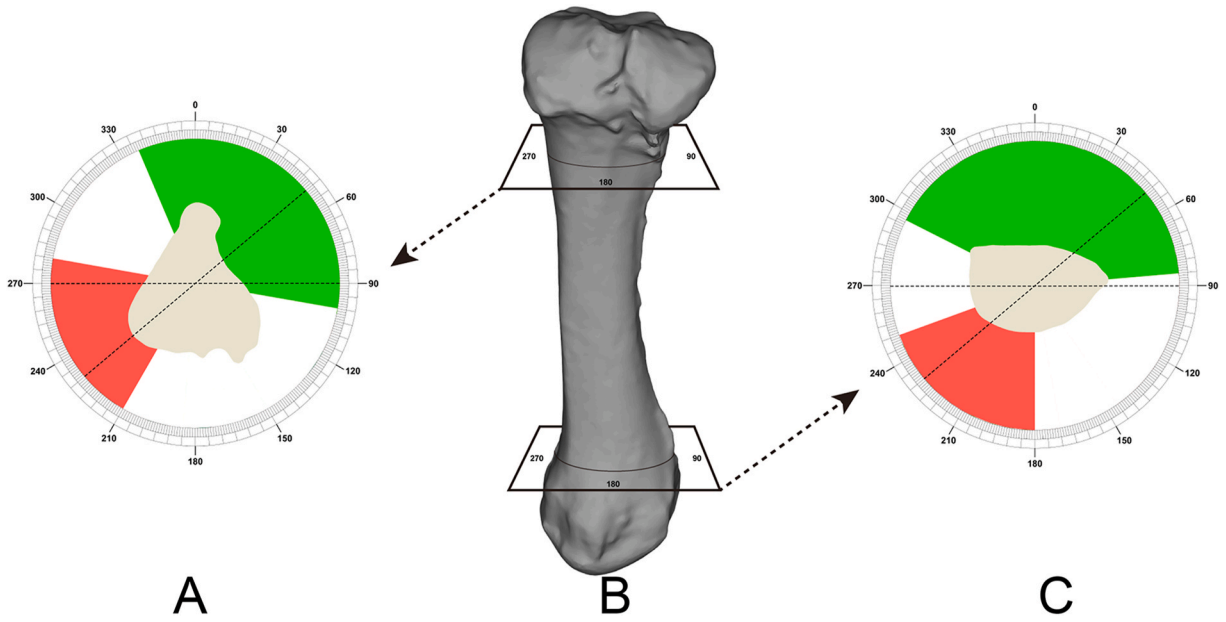

Fig. 7. Safety zone and danger zone in tibia treatment. Green indicates safety zone, red indicates danger zone, and dotted line indicates safe corridor recommended for conventional nail placement. A. Ascending branch region; B. Tibia mode pattern; C. Descending branch region.

anatomical characteristics of the tibial intraosseous artery. Considering that human cadaver specimens are difficult to obtain, suitable animal specimens must be used to conduct relevant experiments. Additionally, to more closely resemble the length, shape, and vascular distribution of the human tibia, these specimens must be derived from large animals, such as sheep, deer, pigs, and dogs.

Throop et al. [18] reported that compared with other animals, the tibia of deer is closer to the human tibia in terms of length and morphology. However, no evidence exists to indicate that the distribution of blood vessels around the tibia of a deer is similar to that of humans, and thus, the tibia of these animals may be unsuitable as a reference in our study. Studies have demonstrated that pig bone is similar to human bone in terms of anatomy, morphology, and healing [13,19]. Kotsougiani et al. [14] showed that similar to humans, the nutrient arteries of the porcine tibia originate from the posterior tibial artery. Therefore, we believe that the tibia of pigs is a suitable alternative model for investigating the tibial intraosseous artery.

4.2. The choice of experimental methods

Owing to its unique physiological structure and clinical significance, the tibial intraosseous artery has always been a focus of research. Almansour et al. [20] identified and described the course and distribution of tibial nutrient arteries using computed tomography of the tibia and suggested that this could help reduce damage to nutrient arteries during clinical treatment. Although this finding was supported by an anatomical study by Anetai et al. [21] on lower-limb specimens from the human body, their study did not find any intraosseous arteries. McKeon et al. [22] used navicular bone with exposed intraosseous arteries by blue latex perfusion and bone transparency and illustrated the arterial blood supply to the navicular bone. However, this transparent model is unable to directly measure intraosseous blood vessels, which does not meet our requirements. Papakonstantinou et al. [23] used the carving method to create humerus specimens with exposed intraosseous arteries. However, this method could not guarantee the integrity of the obtained artery specimens. Zhang et al. [12] provided a method that could fully expose the intraosseous artery and maintain its integrity; this method was employed in the current study. The popliteal artery was isolated and catheterized, and epoxy resin was administered by perfusion to fully expose the intraosseous arteries after acid and alkali corrosion. The three-dimensional distribution of the intraosseous arteries is clearly visible, which is conducive to enhancing the understanding of the intraosseous vasculature and facilitating more direct research on the vessels.

4.3. Intraosseous safe corridor

A safe corridor is defined as an area without any important structures, such as neurovascular bundles, large muscles, and tendons [24]. An intraoperative safe corridor to the tibial shaft portion requires that the implants avoid important tissues such as the anterior tibial vessels, posterior tibial vascular nerve bundle, and peroneal nerve [25]. According to Nayagam [10], the two main safe corridors to the tibial stem are the coronal plane line and the medial line parallel to the subcutaneous medial surface, with an angle of approximately 45° between the two lines. Fixation performed in this manner can ensure stability while reducing the risk of injury to surrounding vessels or nerves. However, if the distribution of blood vessels in the human tibia is similar to that of the porcine tibia, implants with medial line access have a higher probability of damaging the branches of the intraosseous artery in both the proximal and distal ends of the tibial trunk, resulting in a reduced or even interrupted blood supply to a part of the bone cortex (Fig. 7). The distal third of the tibia is supplied only by branches of the nutrient artery and periosteal artery, implying that iatrogenic intraosseous arterial injury may result in delayed healing or non-healing in this region more than in other parts of the tibia [26].

Notably, our findings showed that damage to the trunks of the intraosseous artery could not be avoided by implantation in any direction and angle within a height of approximately 1/10th of the tibia around the midpoint, indicating that implant placement in this area should be avoided as much as possible. Similar conclusions were obtained in a study on the human tibia [27].

Compared to external fixation and plates, intramedullary nailing has shown a lower rate of nonunion in the treatment of closed tibial fractures, which may be related to reduced damage to the soft tissue and extraosseous blood supply [28]. However, the extent of damage caused by intramedullary nailing on the intraosseous blood supply is unclear, and different nailing placement methods and approaches may lead to different degrees of intraosseous vascular injury. A study by Paar et al. [29] on intraosseous vessels in human cadaveric tibial specimens found a 100% rate of intraosseous vessel injury in specimens fixed with reamed intramedullary nailing and 50% in specimens fixed with unreamed intramedullary nailing. Although Menck et al. [30] suggested the use of an intramedullary nail with an improved shape based on a study of human cadaveric tibial specimens, the authors did not explain the distribution pattern of the intraosseous arteries, nor could they confirm that the improved intramedullary nail did indeed reduce or avoid injury to the intraosseous vessels. Our study demonstrated the branches of intraosseous vessels is less distributed in the anterolateral aspect of the tibial medullary cavity, imply that the anterolateral aspect of the tibial medullary cavity may represent a safe corridor for intramedullary nail placement.

4.4. Significance of this study

Many tibial disorders, including nonunion, infection, and necrosis, are associated with blood supply disruption [6,31,32]. Nevertheless, there is still a lack of a clinically appropriate assessment system for the degree of tibial blood supply injury, which is related to our lack of understanding of tibial vasculature. In this study, we clearly demonstrated the structure of the intraosseous tibial artery and summarized its distribution characteristics. Our results may help to gain insight into the components and operating mechanisms of tibial blood circulation and contribute to the development of an assessment method for the degree of blood supply injury.

The safe corridor serves to avoid intraoperative damage to vital structures; however, traditional safe corridors do not focus on the protection of the intraosseous artery. Although further experiments are necessary to verify whether the results of this study can be extrapolated to humans, we can nevertheless propose the novel concept of a safe corridor in the tibia. This concept will not only help in

the intraoperative protection of the intraosseous tibial artery, but will also contribute to the development of novel surgical approaches and instruments to reduce or avoid damage to the intraosseous artery.

The present study has some limitations. First, there is no evidence that the intraosseous artery distribution in the porcine tibia is similar to that in the human tibia, and the results obtained in this investigation may not be directly applicable in clinical practice. Second, because we did not dissect the extraosseous arteries in this study, we could not demonstrate the complete tibial arterial system. Finally, the sample size of this experiment was not large enough to propose typing of intraosseous arteries based on the results obtained. The latter limitation should be addressed in future studies.

5. Conclusion

In this study, we produced an adequate sample of porcine tibial specimens with exposed intraosseous arteries, directly visualized the distribution pattern of porcine intraosseous tibial arteries, and determined the number, course, and location of the arteries. To the best of our knowledge, this is the first study to report these findings. Our results not only deepen our understanding of the intraosseous tibial artery but will also help researchers establish and apply new safe corridors in the future.

Author contributions

Jiaming Wan, Hongyu Wang and Ruixing Hou conceived and designed the experiments. Jiaming Wan and Hongyu Wang performed the experiments. Ruixing Hou, Xiaosong Wang and Dingsong Wang analyzed and interpreted the data. Dingsong Wang and Xiaosong Wang contributed reagents, materials, analysis tools or data. Jiaming Wan and Hongyu Wang wrote the paper. Jiaming Wan and Hongyu Wang contributed equally to this work.

Declaration of competing interest

The authors declare that they have no known competing financial interests or personal relationships that could have appeared to influence the work reported in this paper.

References

[1] R. Tian, F. Zheng, W. Zhao, Y. Zhang, J. Yuan, B. Zhang, L. Li, Prevalence and influencing factors of nonunion in patients with tibial fracture: systematic review and meta-analysis, J. Orthop. Surg. Res. 15 (1) (2020) 377, https://doi.org/10.1186/s13018-020-01904-2.
[2] D. Wennergren, C. Bergdahl, J. Ekelund, H. Juto, M. Sundfeldt, M. Möller, Epidemiology and incidence of tibia fractures in the Swedish fracture register, Injury 49 (11) (2018) 2068–2074, https://doi.org/10.1016/j.injury.2018.09.008.
[3] J.W. Busse, M. Bhandari, S. Sprague, A.P. Johnson-Masotti, A. Gafni, An economic analysis of management strategies for closed and open grade I tibial shaft fractures, Acta Orthop. 76 (5) (2005) 705–712, https://doi.org/10.1080/17453670510041808.
[4] D.W. Shim, H. Hong, K.C. Cho, S.H. Kim, J.W. Lee, S.Y. Sung, Accelerated tibia fracture healing in traumatic brain injury in accordance with increased hematoma formation, BMC Muscoskel. Disord. 23 (1) (2022) 1110, https://doi.org/10.1186/s12891-022-06063-5.
[5] O. Grundnes, O. Reikerås, The importance of the hematoma for fracture healing in rats, Acta Orthop. Scand. 64 (3) (1993) 340–342, https://doi.org/10.3109/17453679308993640.
[6] A.L. Wallace, E.R. Draper, R.K. Strachan, I.D. McCarthy, S.P. Hughes, The effect of devascularisation upon early bone healing in dynamic external fixation, J. Bone Jt. Surg. Br. Vol. 73 (5) (1991) 819–825, https://doi.org/10.1302/0301-620X.73B5.1894674.
[7] G.E. Nelson Jr., P.J. Kelly, L.F. Peterson, J.M. Janes, Blood supply of the human tibia, J. Bone Jt. Surg. Am. Vol. 42-A (1960) 625–636.
[8] L.P. Fischer, J.P. Carret, G.P. Gonon, Vascularisation artérielle du tibia chez l'adulte [Arterial vascularization of the tibia in the adult], Bull. de l'Assoc. des Anatomistes. 59 (167) (1975) 863–875.
[9] S. Hussain, S. Balamoody, S. Wright, D. Bose, P. Fenton, Avoiding iatrogenic vascular injury in tibial external fixation with half pins. An in-vivo study based on CT angiography, J. Clin. Orthopaedics Trauma 25 (2022), 101777, https://doi.org/10.1016/j.jcot.2022.101777.
[10] S. Nayagam, Safe corridors in external fixation: the lower leg (tibia, fibula, hindfoot and forefoot), Strategies Trauma Limb Reconstr. 2 (2-3) (2007) 105–110, https://doi.org/10.1007/s11751-007-0023-7.
[11] F.W. Rhinelander, Tibial blood supply in relation to fracture healing, Clin. Orthop. Relat. Res. (105) (1974) 34–81.
[12] X. Zhang, W. Deng, J. Ju, S. Zhang, H. Wang, K. Geng, D. Wang, G. Zhang, Y. Le, R. Hou, A method to visualize and quantify the intraosseous arteries of the femoral head by vascular corrosion casting, Orthop. Surg. 14 (8) (2022) 1864–1872, https://doi.org/10.1111/os.13319.
[13] A.I. Pearce, R.G. Richards, S. Milz, E. Schneider, S.G. Pearce, Animal models for implant biomaterial research in bone: a review, Eur. Cell. Mater. 13 (2007) 1–10, https://doi.org/10.22203/ecm.v013a01.
[14] D. Kotsougiani, J.I. Willems, A.Y. Shin, P.F. Friedrich, C.A. Hundepool, A.T. Bishop, A new porcine vascularized tibial bone allotransplantation model. Anatomy and surgical technique, Microsurgery 38 (2) (2018) 195–202, https://doi.org/10.1002/micr.30255.
[15] A.K. Gladczak, P.K. Shires, K.A. Stevens, J.W. Clymer, Comparison of indirect and direct blood pressure monitoring in normotensive swine, Res. Vet. Sci. 95 (2) (2013) 699–702, https://doi.org/10.1016/j.rvsc.2013.05.013.
[16] F. Suwa, M. Uemura, A. Takemura, I. Toda, Y.R. Fang, Y.J. Xu, Z.Y. Zhang, Acrylic resin injection method for blood vessel investigations, Okajimas Folia Anat. Jpn. 90 (2) (2013) 23–29, https://doi.org/10.2535/ofaj.90.23.
[17] I. Koshima, T. Yamamoto, M. Narushima, M. Mihara, T. Iida, Perforator flaps and supermicrosurgery, Clin. Plast. Surg. 37 (4) (2010) 683–iii, https://doi.org/10.1016/j.cps.2010.06.009.
[18] A.D. Throop, A.K. Landauer, A.M. Clark, L. Kuxhaus, Cervine tibia morphology and mechanical strength: a suitable tibia model? J. Biomech. Eng. 137 (3) (2015) https://doi.org/10.1115/1.4029302.
[19] M. Thorwarth, S. Schultze-Mosgau, P. Kessler, J. Wiltfang, K.A. Schlegel, Bone regeneration in osseous defects using a resorbable nanoparticular hydroxyapatite, J. Oral Maxillofac. Surg.: Off. J. Am. Assoc. Oral Maxillofacial Surgeons 63 (11) (2005) 1626–1633, https://doi.org/10.1016/j.joms.2005.06.010.
[20] H. Almansour, E. Armoutsis, M.K. Reumann, K. Nikolaou, F. Springer, The anatomy of the tibial nutrient artery canal-an investigation of 106 patients using multi-detector computed tomography, J. Clin. Med. 9 (4) (2020) 1135, https://doi.org/10.3390/jcm9041135.
[21] H. Anetai, S. Kinose, R. Sakamoto, R. Onodera, K. Kato, Y. Kawasaki, T. Miyaki, H. Kudoh, T. Sakai, K. Ichimura, Anatomic characterization of the tibial and fibular nutrient arteries in humans, Anat. Sci. Int. 96 (3) (2021) 378–385, https://doi.org/10.1007/s12565-020-00600-9.
[22] K.E. McKeon, J.J. McCormick, J.E. Johnson, S.E. Klein, Intraosseous and extraosseous arterial anatomy of the adult navicular, Foot Ankle Int. 33 (10) (2012) 857–861, https://doi.org/10.3113/FAI.2012.0857.

[23] M.K. Papakonstantinou, W.R. Pan, C.M. le Roux, M.D. Richardson, New approach to the study of intraosseous vasculature, ANZ J. Surg. 82 (10) (2012) 704–707, https://doi.org/10.1111/j.1445-2197.2012.06142.x.
[24] I. Prackova, V. Paral, M. Kyllar, Safe corridors for external skeletal fixator pin placement in feline long bones, J. Feline Med. Surg. 24 (10) (2022) 1008–1016, https://doi.org/10.1177/1098612X211057329.
[25] M.J. Vives, N.A. Abidi, S.N. Ishikawa, R.V. Taliwal, P.F. Sharkey, Soft tissue injuries with the use of safe corridors for transfixion wire placement during external fixation of distal tibia fractures: an anatomic study, J. Orthop. Trauma 15 (8) (2001) 555–559, https://doi.org/10.1097/00005131-200111000-00004.
[26] E. Santolini, S.D. Goumenos, M. Giannoudi, F. Sanguineti, M. Stella, P.V. Giannoudis, Femoral and tibial blood supply: a trigger for non-union? Injury 45 (11) (2014) 1665–1673, https://doi.org/10.1016/j.injury.2014.09.006.
[27] H. Almansour, J. Jacoby, H. Baumgartner, M.K. Reumann, K. Nikolaou, F. Springer, Injury of the tibial nutrient artery canal during external fixation for lower extremity fractures: a computed tomography study, J. Clin. Med. 9 (7) (2020) 2235, https://doi.org/10.3390/jcm9072235.
[28] N.A. Ebraheim, B. Evans, X. Liu, M. Tanios, M. Gillette, J. Liu, Comparison of intramedullary nail, plate, and external fixation in the treatment of distal tibia nonunions, Int. Orthop. 41 (9) (2017) 1925–1934, https://doi.org/10.1007/s00264-017-3432-3.
[29] O. Paar, D. mon O'Dey, M.N. Magin, A. Prescher, Beeinträchtigung der Arteria nutricia tibiae durch die aufgebohrte und die unaufgebohrte Marknagelung. Untersuchung zur Gefässarchitektur der humanen Tibiamarkhöhle [Disruption of the arteria nutricia tibiae by reamed and unreamed intramedullary nailing. Study of the vascular architecture of the human tibial intramedullary cavity], Zeitschrift fur Orthopadie und ihre Grenzgebiete 138 (1) (2000) 79–84, https://doi.org/10.1055/s-2000-10119.
[30] J. Menck, C. Bertram, J. Grüber, W. Lierse, Entwicklung eines Tibiamarknagels auf der Basis anatomischer Untersuchungen der intraossären Gefässe [Design of a tibial intramedullary nail based on anatomic studies of intraosseous vessels], Unfallchirurgie 18 (6) (1992) 321–324, https://doi.org/10.1007/BF02588365.
[31] I. Oesman, D.H. Adhimukti, Osteonecrosis of the distal tibia in systemic lupus erythematosus: a rare case report, Int. J. Surg. Case Rep. 77 (2020) 126–128, https://doi.org/10.1016/j.ijscr.2020.10.069.
[32] P.M. Rommens, W. Coosemans, P.L. Broos, The difficult healing of segmental fractures of the tibial shaft, Arch. Orthop. Trauma Surg. 108 (4) (1989) 238–242, https://doi.org/10.1007/BF00936208.